A LAYER-WISE FOURIER EXPANSION APPROACH FOR STRESS TRANSFER IN CROSS-PLY LAMINATES WITH TRANSVERSE MATRIX CRACKS

Jian Yang*, Jianqiao Ye**
***Department of Civil Engineering, University of Birmingham, Birmingham, B15 2TT U.K.,**
****School of Civil Engineering, University of Leeds, Leeds, LS2 9JT, U.K**

Keywords: *Fourier expansion, Stress transfer, Laminate, Transverse Matrix Cracks*

Abstract

A method to analyze stress transfer in cross-ply laminates with transverse micro-cracks is presented. The governing equations of the problem are derived on the basis of the plane strain assumption and the two-dimensional equations of elasticity. By using Fourier series expansions, the governing equations are converted to a set of linear algebra equations system. The method takes into account the discontinuities of the series expansions at boundaries. The method is applied to obtain solutions, with which published results can be found for comparisons. Further parametric studies are carried out for cracked laminates with various geometric and material properties.

1 Introduction

Stress transfer in laminated composites with transverse cracks is an important subject in mechanics of composites. Through testing and numerical modeling, it has been recognized that early stage of failure in laminates is dominated by transverse cracking that is initiated by fiber-matrix debonding or/and matrix micro-cracks. Hence, accurate predictions of the stress fields near transverse cracks are fundamentally important for engineers to have a better understanding of damage development in and failure mechanism of laminated structures. As a result, allowance can be given in designs so that an initially damaged laminate can still function satisfactorily as a structural element.

Investigations have been carried out in recent years to study stress field in the vicinity of transverse cracks in laminates. For cross-ply laminates with equally spaced transverse cracks in all or parts of 90 degree plies and subjected to uni-axial forces and bending moments in one direction, McCartney and Pierse [1] proposed an plane strain model that can satisfy the continuity conditions of both tractions and displacements at interfaces between adjacent layers and the 'weighted average' equilibrium equations. The model is also capable of handling through-thickness temperature variations for either symmetrically or non-symmetrically stacked laminate.

On the basis of the same plane strain assumption used by McCartney and Pierse [1], this paper provides an alternative solution to the stress transfer problem. The new solution starts with expressing the longitudinal normal stress of a layer as the sum of the uniform stress due to the layer-wise longitudinal force and the linear stress due to bending. Other stress components are obtained subsequently by solving the two dimensional equilibrium equations of stresses. By imposing the continuity conditions at interfaces and satisfying the stress-displacement relations in the sense of weighted integration, the governing equations of the problem are obtained in terms of the layer-wise longitudinal forces and bending moments. The governing equations are then solved by using the Fourier series expansions. To deal with boundary-discontinuities arising from high order differentials of the series expansions, the technique based on Hobson [2] and Chaudhuri [3] is used. As a consequence, the dimension of final linear algebra equation system depends solely on the number of the layers used in the calculation and is completely independent of the number of terms in the series expansions.

A convergence study is carried out to demonstrate the convergence of the present method when increasing the number of the truncated series and the subdivision of the material layer. Furthermore, to validate the new solution, particularly, in connection with the treatment of boundary discontinuity of Fourier series expansions, comparisons are made in this paper with the results of McCartney and Pierse [1] and Schoeppner and Pagano [4].

2 Basic Equation of Plane Strain Model

Considering a composite laminate having the combination of 0^o and 90^o layers, it is assumed that more than one 90^o plies possibly have transverse cracks in the matrix that run through the entire width along the fiber direction. The cracks are assumed to have the same horizontal location and distributed discontinuously in the thickness direction. It is also assumed that the horizontal distribution of the cracks is equally spaced, so that a representative element in two neighboring cracks can be taken out to predict the stress and displacement fields. It is further assumed that each ply of the laminate is elastic, homogeneous and orthotropic, and the laminate has perfect interlaminar bonding, *i.e.*, there is no delamination.

Fig. 1(a) shows the cross-section of a representative element, where each material layer is further divided into sub-layers, if it is necessary to obtain more accurate results (see also McCartney and Pierse [1]). Without loss of generality, let us assume that the laminate element is composed of N sub-layers. A global rectangular Cartesian co-ordinate system x-y-z is chosen for the element with the origin located at the middle point of the upper surface. The interface between two adjacent layers, e.g., i-th and (i+1)-th layers, is denoted with (i), among which (0) and (N) are for the upper and lower surfaces, respectively. The symbols for the stresses, strains, displacements and material constants for the i-th layer are indicated by an unparenthesized superscript i, while those of the i-th interface are denoted by a parenthesized superscript (i). The thickness of the i-th layer is h^i and the total thickness of the laminate is H. A local coordinate system x^i-y^i is adopted for each sub-layer, with its origin located at its geometric center [Fig 1(b)].

The stress transfer in the laminated element shown in Fig. 1(a) is considered under a combined action of an axial tensile stress, σ, an out-of-plan bending moment, M, and a thermal residual stress. Because the element has been divided into sub-layers, it is reasonable to assume that the axial stresses in each sub-layer varies linearly across its thickness. Due to the fact that the crack length has only a negligible effect on the strain-energy release rate associated with a through-thickness matrix crack that spans the entire width of the ply (Guild et al [5]), a plane strain approximation is considered to be adequate. Hence, the stresses and displacements are independent of z co-ordinate. As a result, we have the following basic equations.

2.1 Governing Equations of the Stress Transfer Problem

Assume that the stress fields for the cracked laminates comprise two components, *i.e.*, the stresses in the undamaged laminates under the same applied loads and the perturbation stresses due to the presence of cracks. Introduce $M^i(x)$ and $N^{(i)}(x)$, respectively, to represent the perturbation bending moment of the i-th layer and the perturbation axial force experienced by all the layers above the i-th interface. Following a similar procedures to which used in McCartney and Pierse [1], the following governing equations can be established:

$$
\begin{aligned}
&-\frac{13(h^i)^2}{60\tilde{E}_y^i}N^{(i-1)''''}(x)-\frac{1}{15}\left[\frac{11(h^{i+1})^2}{4\tilde{E}_y^{i+1}}+\frac{2(h^i)^2}{\tilde{E}_y^i}\right]N^{(i)''''}(x)\\
&-\frac{(h^{i+1})^2}{30\tilde{E}_y^{i+1}}N^{(i+1)''''}(x)-\frac{1}{2}\left(\frac{2\tilde{\nu}_{xy}^i}{\tilde{E}_x^i}-\frac{1}{\tilde{G}_{xy}^i}\right)N^{(i-1)''}(x)\\
&+\frac{1}{2}\left(\frac{1}{\tilde{G}_{xy}^i}-\frac{1}{\tilde{G}_{xy}^{i+1}}\right)N^{(i)''}(x)+\frac{1}{2}\left(\frac{2\tilde{\nu}_{xy}^{i+1}}{\tilde{E}_x^{i+1}}-\frac{1}{\tilde{G}_{xy}^{i+1}}\right)N^{(i+1)''}(x)\\
&+\frac{13h^i}{35\tilde{E}_y^i}M^{i''''}(x)+\frac{9h^{i+1}}{70\tilde{E}_y^{i+1}}M^{i+1''''}(x)\\
&+\frac{6}{5h^i}\left(\frac{2\tilde{\nu}_{xy}^i}{\tilde{E}_x^i}-\frac{1}{\tilde{G}_{xy}^i}\right)M^{i''}(x)-\frac{6}{5h^{i+1}}\left(\frac{2\tilde{\nu}_{xy}^{i+1}}{\tilde{E}_x^{i+1}}-\frac{1}{\tilde{G}_{xy}^{i+1}}\right)M^{i+1''}(x)\\
&+\frac{12}{(h^i)^3\tilde{E}_x^i}M^i(x)-\frac{12}{(h^{i+1})^3\tilde{E}_x^{i+1}}M^{i+1}(x)\\
&-\frac{h^i}{2\tilde{E}_y^i}\sigma_y^{(i-1)''}(x)-\frac{h^{i+1}}{2\tilde{E}_y^{i+1}}\sigma_y^{(i)''}(x)=0\\
&\qquad i=1,2,\ldots,N-1 \qquad (1)
\end{aligned}
$$

$$
\begin{aligned}
&\frac{(h^i)^3}{30\tilde{E}_y^i}N^{(i-1)''''}(x)+\frac{1}{20}\left[\frac{(h^i)^3}{3\tilde{E}_y^i}-\frac{(h^{i+1})^3}{2\tilde{E}_y^{i+1}}\right]N^{(i)''''}(x)\\
&-\frac{(h^{i+1})^2}{120\tilde{E}_y^{i+1}}N^{(i+1)''''}(x)+\frac{h^i}{12}\left(\frac{8\tilde{\nu}_{xy}^i}{\tilde{E}_x^i}-\frac{1}{\tilde{G}_{xy}^i}\right)N^{(i-1)''}(x)\\
&+\left[\frac{h^i}{12}\left(\frac{4\tilde{\nu}_{xy}^i}{\tilde{E}_x^i}+\frac{1}{\tilde{G}_{xy}^i}\right)-\frac{h^{i+1}}{12}\left(\frac{2\tilde{\nu}_{xy}^{i+1}}{\tilde{E}_x^{i+1}}-\frac{1}{\tilde{G}_{xy}^{i+1}}\right)\right]N^{(i)''}(x)\\
&+\frac{h^{i+1}}{12}\left(\frac{2\tilde{\nu}_{xy}^{i+1}}{\tilde{E}_x^{i+1}}-\frac{1}{\tilde{G}_{xy}^{i+1}}\right)N^{(i+1)''}(x)+\frac{1}{h^i\tilde{E}_y^i}N^{(i-1)}(x)\\
&-\left(\frac{1}{h^i\tilde{E}_y^i}+\frac{1}{h^{i+1}\tilde{E}_y^{i+1}}\right)N^{(i)}(x)+\frac{1}{h^{i+1}\tilde{E}_y^{i+1}}N^{(i+1)}(x)
\end{aligned}
$$

$$
\begin{aligned}
&-\frac{11\left(h^i\right)^2}{210\tilde{E}_y^i}M^{i''''}(x)+\frac{13\left(h^{i+1}\right)^2}{420\tilde{E}_y^{i+1}}M^{i+1''''}(x) \\
&-\frac{3}{5}\left(\frac{12\tilde{\nu}_{xy}^i}{\tilde{E}_x^i}-\frac{1}{\tilde{G}_{xy}^i}\right)M^{i''}(x)-\frac{1}{10}\left(\frac{2\tilde{\nu}_{xy}^{i+1}}{\tilde{E}_x^{i+1}}-\frac{1}{\tilde{G}_{xy}^{i+1}}\right)M^{i+1''}(x) \\
&-\frac{6}{\left(h^i\right)^2\tilde{E}_x^i}M^i(x)-\frac{6}{\left(h^{i+1}\right)^2\tilde{E}_x^{i+1}}M^{i+1}(x)+\frac{\left(h^i\right)^2}{12\tilde{E}_y^i}\sigma_y^{(i-1)''}(x) \\
&-\frac{\left(h^{i+1}\right)^2}{12\tilde{E}_y^{i+1}}\sigma_y^{(i)''}(x)+\frac{\tilde{\nu}_{xy}^i}{\tilde{E}_x^i}\sigma_y^{(i-1)}(x)-\frac{\tilde{\nu}_{xy}^{i+1}}{\tilde{E}_y^{i+1}}\sigma_y^{(i)}(x)=0 \\
&\qquad i=1,2,\ldots,N-1 \qquad (2)
\end{aligned}
$$

where

$$
\tilde{E}_x^i=\frac{E_x^i}{1-\nu_{xz}^i\nu_{zx}^i};\ \tilde{E}_y^i=\frac{E_y^i}{1-\nu_{yz}^i\nu_{zy}^i};\ \tilde{\nu}_{xy}^i=\frac{\nu_{xy}^i+\nu_{xz}^i\nu_{zy}^i}{1-\nu_{xz}^i\nu_{zx}^i};
$$

$$
\tilde{\alpha}_x^i=\alpha_x^i+\nu_{zx}^i\alpha_z^i;\ \tilde{\alpha}_y^i=\alpha_y^i+\nu_{zy}^i\alpha_z^i \qquad (3)
$$

E_ξ^i and α_ξ^i (ξ=x, y) denote the respective Young's modulus and thermal expansion coefficient of the i-th layer, respectively; $G_{\xi\varsigma}^i$ and $\nu_{\xi\varsigma}^i$ (ξ, ς =x, y, z) denote the shear modulus and Poisson's ratio in ξ-ς plane, respectively; ΔT^i is the difference between the current temperature and the stress-free temperature of the laminate in the i-th layer. In this paper, it is assumed that the temperature is independent of x co-ordinate.

Applying the boundary conditions, we obtain

$$
N^{(i)'}(\pm L)=0;\quad M^{i'}(\pm L)=0,\quad i=1\ ..\ N\text{-}1 \qquad (4)
$$

For the cracked layers,

$$
M^i(\pm L)=-\frac{1}{12}\left(h^i\right)^3E_x^i\hat{\varepsilon};
$$

$$
N^{(i)}(\pm L)-N^{(i-1)}(\pm L)=-h^iE_x^i\left[\varepsilon+\left(Y^{(i)}-\frac{h^i}{2}\right)\hat{\varepsilon}-\tilde{\alpha}_x^i\Delta T^i\right] \qquad (5a,\ b)
$$

For the uncracked layers, the boundary conditions can be obtained by considering weighted integrations of the longitudinal displacements, i.e.

$$
\int_{Y^{(i-1)}}^{Y^{(i)}}U^i(\pm L,y)\left(1,\frac{y}{h^i}\right)\frac{dy}{h^i}=\pm\int_{Y^{(i-1)}}^{Y^{(i)}}(\varepsilon_c+\hat{\varepsilon}_c y)L\left(1,\frac{y}{h^i}\right)dy \qquad (6)
$$

where ε and $\hat{\varepsilon}$ are the parameters that characterize the axial strain and bending of the relative uncracked laminate, which can be determined by using the classic laminate theory (CLT).

If the N-th layer is assumed uncracked. Eq. 6 lead to

$$
\frac{\int_0^{\pm L}M^i(p)dp}{\left(h^i\right)^3\tilde{E}_x^i}-\frac{\int_0^{\pm L}M^N(p)dp}{\left(h^N\right)^3\tilde{E}_x^N}=0,\qquad (i\neq N) \qquad (7a)
$$

$$
\begin{aligned}
&\frac{\int_0^{\pm L}N^{(i)}(p)dp-\int_0^{\pm L}N^{(i-1)}(p)dp}{h^i\tilde{E}_x^i} \\
&-\frac{\int_0^{\pm L}N^{(N)}(p)dp-\int_0^{\pm L}N^{(N-1)}(p)dp}{h^N\tilde{E}_x^N}+\frac{12\int_0^{\pm L}M^i(p)dp}{\left(h^i\right)^3\tilde{E}_x^i}\left(Y^{(i)}-\frac{h^i}{2}\right) \\
&-\frac{12\int_0^{\pm L}M^N(p)dp}{\left(h^N\right)^3\tilde{E}_x^N}\left(H-\frac{h^N}{2}\right)=0,\quad (i\neq N) \qquad (7b)
\end{aligned}
$$

Free tractions conditions on the top and bottom surfaces lead to

$$
N^{(0)}(x)=0;\qquad N^{(N)}(x)=0;
$$

$$
M^{N''}(x)=\sum_{j=1}^{N-1}\left[\frac{\left(h^j+h^{j+1}\right)}{2}N^{(j)''}(x)-M^{j''}(x)\right] \qquad (8a\text{-}c)
$$

In addition, the interfacial stresses can be expressed in terms of $N^{(i)}(x)$ and $M^i(x)$ as

$$
\sigma_{xy}^{(i)}(x)=-N^{(i)'}(x);
$$

$$
\sigma_y^{(i)}(x)=\sum_{j=1}^{i}\left[\frac{\left(h^j+h^{j+1}\right)}{2}N^{(j)''}(x)-M^{j''}(x)\right]-\frac{h^{i+1}}{2}N^{(i)''}(x)
$$

$$
i=1,\ \ldots,\ N-1 \qquad (9a,b)
$$

2.2 Solution of the Governing Equations

The solution of the 2(N-1) simultaneous differential Eqs. (1) and (2) is assumed in the form of following Fourier series expansion (for the sake of symmetry, the axial force and bending moment are only expanded in $[0,L]$):

$$
N^{(i)}(x)=\sum_{m=0}^{\infty}a_m^{(i)}\cos\left(\frac{m\pi}{L}x\right);
$$

$$
M^i(x)=\sum_{m=0}^{\infty}b_m^i\cos\left(\frac{m\pi}{L}x\right)
$$

$$
x\in[0,L] \qquad (10\ a,\ b)
$$

The 1st and 2nd differentiations of the assumed solutions (9) can be obtained by differentiating the Fourier series term-wisely in the whole domain, while the boundary-discontinuities arose for the 3rd differentiations, so the technique due to Hobson [2] and Chaudhuri [3] is used and it yields

$$
N^{(i)'''}(x)=\frac{\pi^3}{L^3}\sum_{m=1}^{\infty}a_m^{(i)}m^3\sin\left(\frac{m\pi}{L}x\right)\quad x\in[0,L)\ \text{and}
$$

$$
N^{(i)'''}(L)=N_L^{(i)} \qquad (11a)
$$

$$
M^{i'''}(x)=\frac{\pi^3}{L^3}\sum_{m=1}^{\infty}b_m^im^3\sin\left(\frac{m\pi}{L}x\right)\quad x\in[0,L)\ \text{and}
$$

$$
M^{i'''}(L)=M_L^i \qquad (11b)
$$

$$N^{(i)''''}(x)=\frac{N_L^{(i)}}{L}+\sum_{m=1}^{\infty}\left[\frac{2N_L^{(i)}}{L}(-1)^m+\frac{\pi^4}{L^4}a_m^{(i)}m^4\right]\cos\left(\frac{m\pi}{L}x\right)$$

$$x\in[0,L) \tag{11c}$$

$$M^{i''''}(x)=\frac{M_L^i}{L}+\sum_{m=1}^{\infty}\left[\frac{2M_L^i}{L}(-1)^m+\frac{\pi^4}{L^4}b_m^{(i)}m^4\right]\cos\left(\frac{m\pi}{L}x\right)$$

$$x\in[0,L) \tag{11d}$$

where $N_L^{(i)}$ and M_L^i are unknown constants that represent the values of the third derivatives of axial force and bending moment at x=L, respectively and at the same point, their 4th derivatives are nonexistent.

Substituting Eqs (10) and (11) into governing Eqs (1) and (2) yields the following matrix equation:

$$\mathbf{a_m}=-\mathbf{A_m^{-1}B_m b} \tag{12}$$

where

$$\mathbf{a_m}=\{a_m^{(1)},b_m^1,\cdots,a_m^{(N-1)},b_m^{N-1}\}^T;$$

$$\mathbf{b}=\{N_L^{(1)},M_L^1,\cdots,N_L^{(N-1)},M_L^{N-1}\}^T;$$

$$\mathbf{B_m}=\begin{cases}\frac{1}{2}\mathbf{B} & m=0\\ (-1)^m\mathbf{B} & m\neq 0\end{cases} \tag{13a-c}$$

$\mathbf{A_m}$ and $\mathbf{B}$ are matrices relative to the m-th term of the Fourier expansions and their elements can be expressed explicitly in terms of the geometric and material parameters of the laminate. For the sake of simplicity, these expressions are not given here.

It can be seen that the boundary conditions shown by Eqs (4) are satisfied automatically. After introducing Eqs (11) into boundary conditions (5) and (7), a set of linear algebra equations in terms of $\mathbf{a_m}$ is obtained. The elimination of $\mathbf{a_m}$ using Eq (12) leads to

$$\mathbf{Db}=-\mathbf{c} \tag{14}$$

where

$$\mathbf{D}=\frac{1}{2}\mathbf{C_0A_0^{-1}B}+\mathbf{C}\sum_{m=1}^{\infty}\mathbf{A_m^{-1}B} \tag{15}$$

$\mathbf{C_0}$, and $\mathbf{C}$ are the matrices relative to the cases when $m=0$ and $m\neq 0$, respectively. The column matrix c consists of the contributions from the right-hand sides of Eqs (5) and (7). The elements of these three matrices can also be represented explicitly in a general form.

From Eq (13c) and Eq (14) , we can obtain

$$\mathbf{a_m}=\begin{cases}\frac{1}{2}\mathbf{A_0^{-1}BD^{-1}c} & m=0\\ (-1)^m\mathbf{A_m^{-1}BD^{-1}c} & m\neq 0\end{cases} \tag{15}$$

After solving for $\mathbf{b}$ and then $\mathbf{a_m}$, $N^{(i)}(x)$ and $M^{(i)}(x)$ are calculated using Eqs (10) and, subsequently, all the stresses can be found.

3 Convergent Study and Validating Example

To demonstrate the convergence of the present method, a study of the interfacial stresses for the [0^o/90^o]$_S$ E-glass fiber/Epoxy laminate (Soden et al. [6]) given in Table 1, subjected to a combination of a uni-axial stress of σ = 1.0 GPa, a bending moment of M = 1.0 KN and a uniform thermal load of ΔT = -100^o, are carried out for a crack separation space 2L = 5 mm and an equal ply thickness h_{ply} = 0.25mm. The results are presented in Fig. 2, where the dimensionless interfacial shear (σ_{xy}/σ^*) and normal (σ_y/σ^*) stresses along the interface between the lower 0^o and 90^o plies. Here σ^* denotes the maximum longitudinal stress in the bottom fibers of the corresponding uncracked laminate subjected to the same mechanical and thermal loads and is 1.451GPa herein. Fig. 2 shows the effects of the truncated series expansions and the subdivision of the material layer upon the interfacial stresses. In the figure, N_{tru} denotes the number of the Fourier terms used in the calculation; N_{ply} denotes the number of sublayers of an initial division in each of the material plies and N_{ref} is a number related to further refinement in the sub-layers next to the interfaces, e.g, N_{ref} =3 means that the two sub-layers neighboring an interface are, respectively, divided into three layers. From the figures, it can be seen that the normal stress converges faster than shear stress. By using up to 300 harmonic terms, 5 layer in each ply and further 3 sublayers in the layers next to the interface, Fig. 2(c) presents a smooth distribution of both normal and shear stresses.

As a part of validation of the present method, the interfacial shear and normal stresses at the interface between 0^o and 90^o plies for a four ply ([0^o/90^o]$_S$) Graphite/Epoxy laminate are calculated and compared with the results obtained by McCartney and Pierse [1] and Schoeppner and Pagano [4]. The laminate is subjected to a uni-axial stress of σ = 0.2 Gpa and a uniform thermal load of ΔT = -120$^{o.}$. The material properties used in the calculations are for the graphite/epoxy laminates (Groves et al. [7]) given in Table 1. The geometric parameters are L = 2.0 mm and h_{ply} = 0.25 mm. In the calculation each ply is further divided into five sub-layers of equal thickness. Figs. 3 shows that the results obtained have excellent agreement with those from the alternative methods.

Table 1. Mechanical and thermal properties of the laminae (transversely isotropic material)

Source	Soden et al. [6]	Grovers et al. [7]
Fiber type	Silenka E-Glass 1200tex	Graphite
Matrix type	MY750/HY917/ DY063 Epoxy	Epoxy
Longitudinal modulus, E_x (GPa)	45.6	144.78
Transverse modulus, E_z (GPa)	16.2	9.58
In-plane shear modulus, G_{xz} (GPa)	5.83	4.785
Major Poisson's ratio, ν_{xz} (GPa)	0.278	0.31
Through thickness Poisson's ratio, ν_{zy} (GPa)	0.4	0.55
Longitudinal thermal coefficient, α_x (10^{-6}/^{o}C)	8.6	-0.72
Transverse thermal coefficient, α_z (10^{-6}/^{o}C)	26.4	27.0

4 Concluding Remarks

A new method based on a layer-wise Fourier series approximation has been proposed to investigate the stress transfer in cross ply laminates with transverse matrix cracks. A plane strain representative element was used in the analysis. Because of the use of Fourier expansion, the differential governing equations of the problem were converted to a set of linear algebra equations that can be solved effectively by using existing algorisms. As a consequence, the new method is more suitable for the analysis of laminates with a large number of material layers or/and when the layer refinement technique is used.

The convergent rate of the new method was assessed with respect to the number of Fourier terms used in the expansion as well as layer refinement in the vicinity of the crack tips. In general, the convergent of interfacial normal stresses is faster than that of the interfacial shear stresses. As the number of terms in the series increases, both stresses approximate the singular behavior near the crack tips.

Comparisons were made between the present results and the results published elsewhere in the literature. Excellent agreement was observed.

References

[1] MaCartney LN, Pierse C. Stress transfer mechanics for multiple ply laminates subject to bending. NPL report CMMT(A) 55, 1997.

[2] Hobson EW. The theory of functions of a real variable and the theory of Fourier's sSeries, 2nd edn, Vol. 2. Cambridge, 1926.

[3] Chaudhuri RA. On boundary-discontinuous double Fourier series solution to a system of completely coupled P.D.E.'s. Int. J. Engng. Sci. 1989; 27(9): 1005-1022.

[4] Schoeppner GA, Pagano NJ. Stress fields and energy release rates in cross-ply laminates. Int. J. Solids Structures 1998; 35(11): 1025-1055.

[5] Guild GJ, Ogin SL, Smith PA. Modeling of 90^o ply cracking in cross ply laminates, including three-dimensional effects. J. Compos. Mater. 1993; 27: 646-667.

[6] Soden PD, Hinton MJ, Kaddour AS. Lamina properties, lay-up configurations and loading conditions for a range of fiber-reinforced composite laminates. Composites Science and Technology 1998; 58: 1011-1022.

[7] Groves SE, Harris CE, Highsmith AL, Allen DH, Norvell RG. An experimental and analytical treatment of matrix cracking in cross-ply laminates. Experimental Mechanics 1987; 27: 73-79.

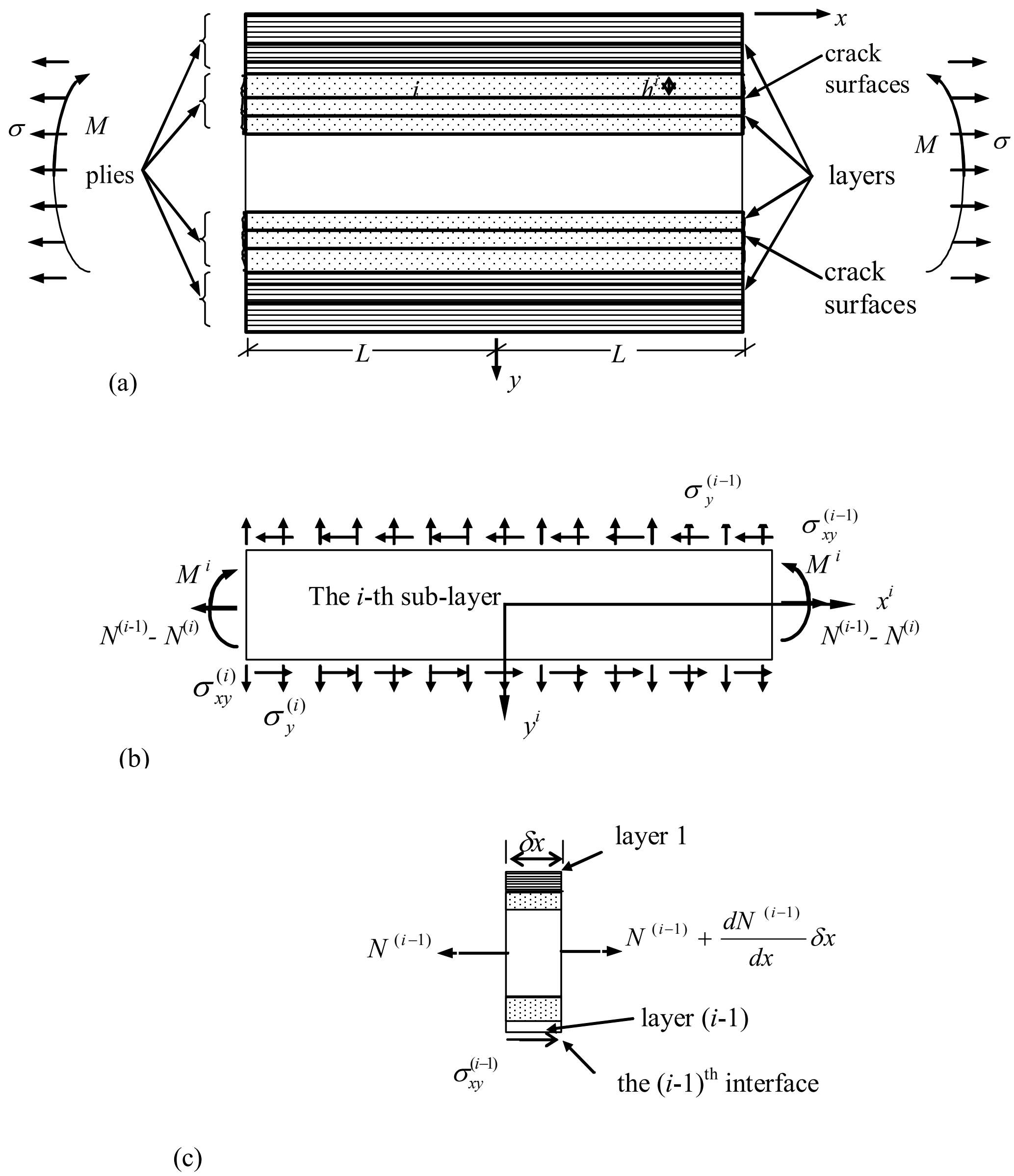

Fig.1 A representative laminated element: (a) The Schematic illustration of a typical element between two neighboring cracked planes; (b) The i-th sub-layer; (c) equilibrium of the layers above the (i-1) th interface

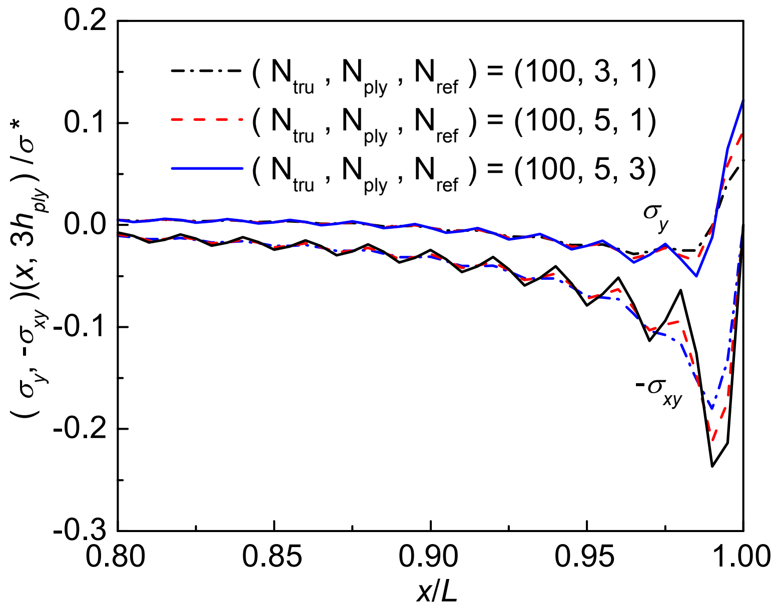
(N_tru , N_ply , N_ref) = (100, 3, 1)
(N_tru , N_ply , N_ref) = (100, 5, 1)
(N_tru , N_ply , N_ref) = (100, 5, 3)
σ_y
-σ_xy
(σ_y, -σ_xy)(x, 3h_ply) /σ*
x/L
0.2
0.1
0.0
-0.1
-0.2
-0.3
0.80
0.85
0.90
0.95
1.00

(a)

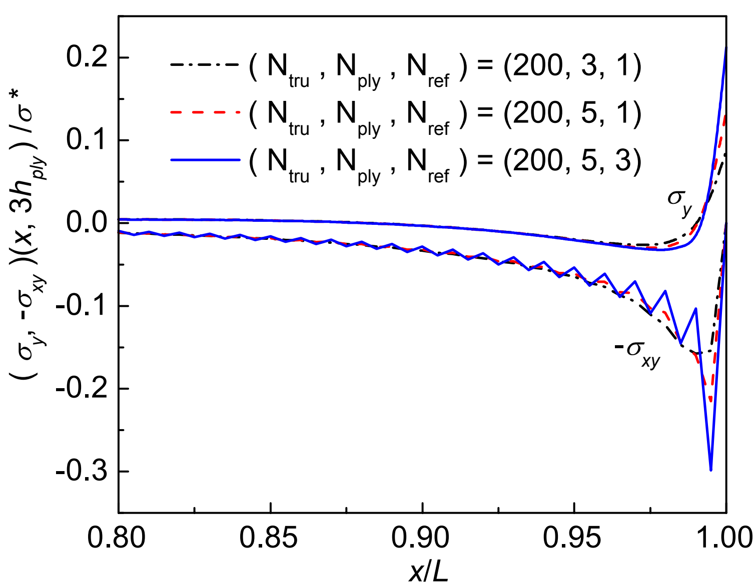
(N_tru , N_ply , N_ref) = (200, 3, 1)
(N_tru , N_ply , N_ref) = (200, 5, 1)
(N_tru , N_ply , N_ref) = (200, 5, 3)
σ_y
-σ_xy
(σ_y, -σ_xy)(x, 3h_ply) /σ*
x/L
0.2
0.1
0.0
-0.1
-0.2
-0.3
0.80
0.85
0.90
0.95
1.00

(b)

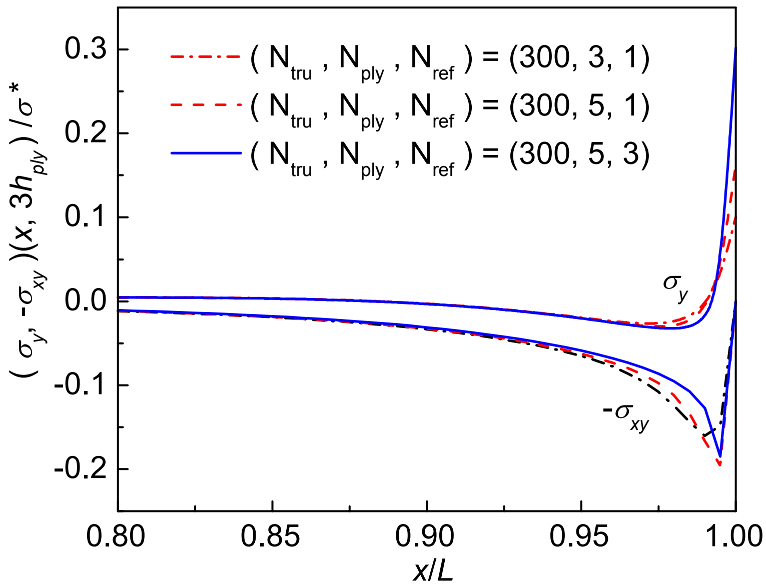

(c)

Fig. 2 Convergence study for the dimensionless interfacial stresses for the $[0/90]_S$ E-glass fiber/Epoxy laminate

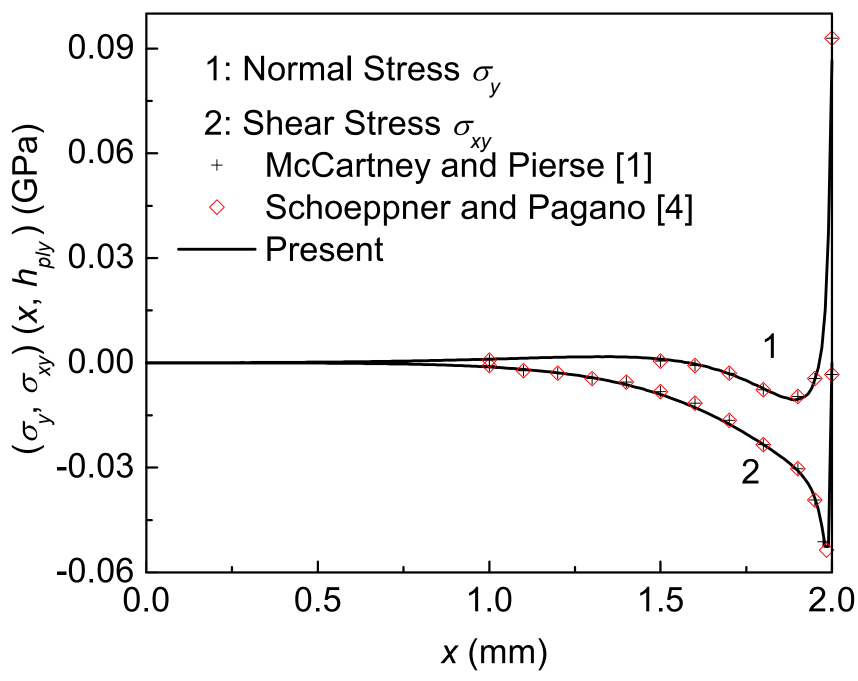

Fig. 3 Comparisons of the interfacial shear stress σ_{xy} and normal stress σ_y in the $[0/90]_S$ Graphite/Epoxy laminate